Freezing out all-optical poling dynamics of azophenylcarbazole molecules in polycarbonate

ARTICLE *in* PHYSICAL CHEMISTRY CHEMICAL PHYSICS · JULY 2013

Impact Factor: 4.49 · DOI: 10.1039/c3cp51918j · Source: PubMed

5 AUTHORS, INCLUDING:

Gediminas Seniutinas
Swinburne University of Technology
51 PUBLICATIONS **199** CITATIONS
SEE PROFILE

Raimondas Petruškevičius
Center for Physical Sciences and Technology
68 PUBLICATIONS **95** CITATIONS
SEE PROFILE

Vytautas Getautis
Kaunas University of Technology
119 PUBLICATIONS **646** CITATIONS
SEE PROFILE

PCCP

RSC Publishing

PAPER

Freezing out all-optical poling dynamics of azophenylcarbazole molecules in polycarbonate†

Cite this: *Phys. Chem. Chem. Phys.*, 2013, **15**, 14219

Gediminas Seniutinas,[a] Armandas Balčytis,[a] Roland Tomašiūnas,*[a] Raimondas Petruškevičius[b] and Vytautas Getautis[c]

Received 6th May 2013,
Accepted 21st June 2013

DOI: 10.1039/c3cp51918j

www.rsc.org/pccp

In this work we have extended the application of a theoretical model describing the processes of all-optical poling of isomerizable molecules while taking into consideration the thermoisomerization related findings presented in the literature. A model describing all-optical poling transients using a three relaxation rate approach was contrasted with the experimental results of azophenylcarbazole doped polycarbonate measured in a wide range of temperatures from 150 to 300 K, thus covering the β transition for the host. By means of a long timescale and low temperature, we were able to better resolve the thermoisomerization and orientational diffusion processes. The *cis* → *trans* thermoisomerization relaxation rates k_1 and k_2 were obtained in the range 10^{-5} to 10^{-2} s^{-1} and the relaxation rate k_3 of the orientational diffusion of the *trans* isomer in the range 10^{-6} to 10^{-4} s^{-1}. The rates exhibited diverse temperature dependent behaviors: the two lowest (k_2,k_3) manifested Arrhenius type dependencies (E_{k_2} = 157 meV), whereas, the highest (k_1) showed a temperature dependence that is non-Arrhenius, or undistinguished for our experimental conditions. The latter was interpreted using the geometrical ''adjustment'' model. By investigating chromophore–polymer systems at temperatures far below T_g, we were able to uncover the situation when the *cis* → *trans* transition is switched-off and the orientational randomization is suppressed. Thus, we could consider the chromophores as ''frozen''.

1 Introduction

Empirical and theoretical discussions about temperature driven relaxation mechanisms in polymers carry back to the fifties and sixties. At that time, not only polymer systems, but also a variety of organic and inorganic glass-forming liquids over a wide temperature range above the vitrification point were examined.[1] Although great experimental, theoretical and simulation efforts made toward a better understanding, the glass transition still remains a perplexing problem.[2] The lack of consensus between theories and models (*e.g.* the free volume theory,[3] the Adam–Gibbs theory,[4] the coupling mode theory,[5] the coupling model,[6] the energy landscape model,[7] and the spatially heterogeneous dynamics[8]) stems greatly from the fact that no experimental technique supports one specific approach. Accordingly, molecular simulation became an essential tool to link theory and experiment. Moreover, atomistic simulation came into play for the glass transition phenomena,[9] however, not always considered as suitable.[10] In fact, as the polymeric system cools down, the available number of configurations decreases, resulting in an increase in the correlation length and a non-Arrhenius behavior of the relaxation time.[11] The Arrhenius relation occurs at a high temperature when the activation energy is the same for all the segments. The problem becomes more complex when two or more subsystems are considered, *e.g.* host–guest systems. Thermodynamics of the polymeric environment plays a crucial role in the temperature and temporal stability of the spatial organization of embedded chromophores. In particular, azo chromophores, which undergo a photochemical interconversion between the *trans* and *cis* configurations. Different spatial arrangements and ground state energies are typical features of these isomers. Besides the photoinduced reversible *trans* → *cis* and *cis* → *trans* isomerizations, a thermally induced *cis* → *trans* back isomerization is exclusively important for controlling the isomerization cycles in molecular switching applications.[12] Thermally induced *cis* → *trans* isomerization was investigated and the activation energy was elucidated for azobenzene derivatives using absorbance[13] and two-photon photoemission spectroscopy measurements.[14] In the simulation of thermal phenomena, most of them used an Arrhenius relation.

[a] *Institute of Applied Research, Vilnius University, Saulėtekio 10, LT-10223 Vilnius, Lithuania. E-mail: rolandas.tomasiunas@ff.vu.lt; Tel: +370 5 2366069*

[b] *Center for Physical Sciences and Technology, Savanoriu av. 231, 02300 Vilnius, Lithuania*

[c] *Kaunas University of Technology, Radvilėnu pl. 19, LT-50270 Kaunas, Lithuania*

† Electronic supplementary information (ESI) available. See DOI: 10.1039/c3cp51918j

Numerous groups that have investigated the processes of isomerization of azo-dyes in polymer matrices report that *cis* → *trans* thermoisomerization transients typically proceed with at least two different rates.[15–17] Understanding the nature of the *cis* → *trans* thermoisomerization is important for studying the dynamics of the induced second order nonlinear susceptibility in azo-dye doped polymers.[18–20] We have extended the application of the theoretical model describing the process of all-optical poling of isomerizable molecules in order to take into consideration the thermoisomerization related findings presented in the literature. The mechanism of the angular redistribution of chromophores during all-optical poling (which could be due to the thermal orientational diffusion of the photoisomer, or to rotation-in-isomerization processes) is another origin of controversy between the different theoretical models. By also including terms for the rotation-in-isomerization and the thermal angular diffusion, we are able to determine the relative influence of these processes and to achieve a more complete theoretical understanding of the evolution of induced non-centrosymmetry in chromophore doped rigid polymer matrix systems. In order to verify the predictions made by our model, simulation results were contrasted to experimental all-optical poling transients of azophenylcarbazole doped polycarbonate measured in a broad range of temperatures.

In the literature we find some works devoted to similar all-optical poling investigations, however, concerned mainly with the intensification of photoinduced reorientation of molecules with temperature increase towards T_g (azobenzene–polyimide,[21] crosslinkable polymer hexamethoxymethyl melamine–DR1 (Disperse Red 1)[22]). An all-aromatic azo chromophore has a higher thermal stability than the alkyl-linked azo chromophore (*e.g.* DR1), thus, also an improved optical stability.[23] Non-centrosymmetry of the media containing the carbazole chromophores was achieved while applying an external electric field (corona poling).[24–27] Despite the effectiveness to align chromophores with a steady-state electric field, the contactless all-optical poling method has many advantages. The quasi-phase matched condition for the optical generation of harmonics (*e.g.* second), or the measurement of the time resolved dynamics of polar media are noteworthy.[28] On the example of two azophenylcarbazole samples consisting of different donor arrangements by means of experiment and simulation, we show how temperature reduces the *cis* → *trans* back isomerization and reorientation of the chromophores.

2 Material and methods

2.1 Characterization of chromophores

The synthetic procedure and corresponding optical and chemical characterization of the azophenylcarbazole-based dyes 3-(4-nitrophenyl)azo-9-propyl-2-propoxy-9*H*-carbazole (**3**, $C_{24}H_{24}N_4O_3$) and 3-(4-nitrophenyl)azo-9-(2-ethyl)hexyl-2-(2-ethyl)hexyloxy-9*H*-carbazole (**4**, $C_{34}H_{44}N_4O_3$) is presented in our former work (see the text and Fig. 1 and 2 in ref. 29). To learn about the optical absorption temperature dependence at quantum energies used for poling, the absorption of second harmonic light in the temperature range 140 to 300 K was measured (Fig. 1). A two-photon absorption threshold used as a measure for optical poling was evaluated from the first harmonic transmission (decrease) dependence on the excitation fluence (Fig. 2).

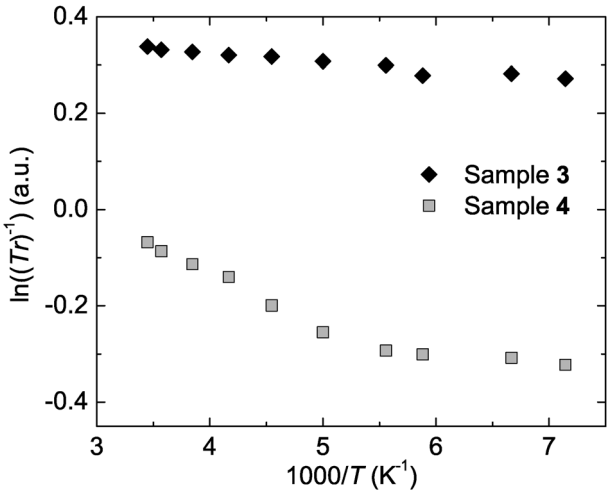

Fig. 1 Temperature dependence of the second harmonic light absorbance of the azophenylcarbazole samples.

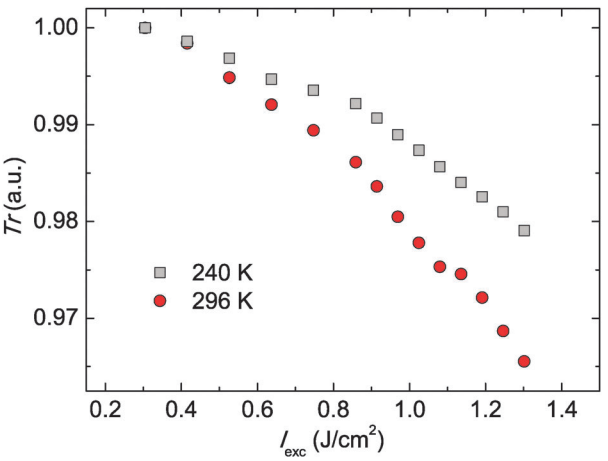

Fig. 2 First harmonic light transmission dependence on the excitation intensity of the azophenylcarbazole sample **4**.

2.2 Preparation of films

Two azophenylcarbazole samples **3** and **4** (Fig. 3) were dispersed in a polycarbonate matrix for the optical poling experiments. The samples were prepared by a spin-coating technique involving a 500 cycles per min spin for the first 6 seconds, followed by a 2000 cycles per min spin for the next 20 seconds. Silica glass plates were used as substrates and were degreased in ethanol, washed in distilled water and dried. Polycarbonate Iupilon Z-200 with a T_g = 189 °C was chosen as the polymer matrix for these molecules to create a guest–host system.

In order to avoid aggregation, the loading density of the chromophores in all the samples was chosen as 10% (wt%).

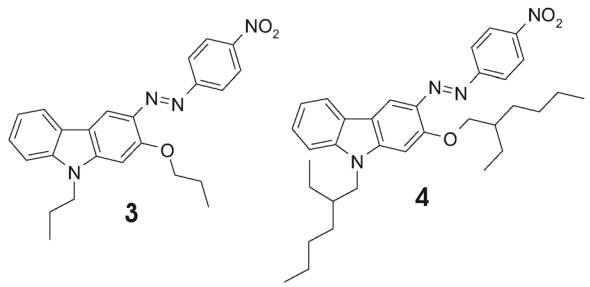

Fig. 3 Molecular structures of the azophenylcarbazole samples **3** and **4**.

Drying *via* two steps (25 min at room temperature followed by 45 min at 80 °C) was performed for finishing.

2.3 Technique for optical poling

A photoinduced molecular orientation process in media containing molecules with azo junctions is able to undergo *trans* → *cis* → *trans* photonically and thermally induced isomerization cycles followed by a change of the orientation of the chromophores toward the perpendicular direction with respect to the polarization of light, or in brief, angular hole burning.[18] If a material with an initial centrosymmetric orientational structure is irradiated with fundamental ω and its second harmonic 2ω beams that fall within its absorption band, quantum interference between the two-photon absorption of the fundamental and one-photon absorption of the second harmonic can be achieved. The coherent pumping of the NLO polymer film results in an orientational hole burning.[28,29] Thus, provided there is a phase difference between these seeding beams, an orientationally selective poling electric field inside the material is established. The orientational hole burning is followed by a reversible *trans* → *cis* → *trans* isomerization process, which drives an optical orientation motion. Finally, it leads to a net permanent molecular polar order. This induced molecular orientation breaks the initial centrosymmetry of the structure inside the material creating a quasi-phase-matched grating of nonlinear second order susceptibility, suitable for second harmonic generation. The highest poling yield is achieved when the polarization of both the seeding beams is linear and aligned parallel to each other, with intensities tuned in a way that the probability for the material to absorb one second harmonic photon and two fundamental frequency photons is the same.[28] We used a two-branch experimental setup.[30] The light source was a Nd:YAG laser (1064 nm, 20 ns, 10 Hz). From the two branches, frequency doubled (2ω) and first harmonic (ω) beams served as the seeding beams. These two beams of a Gaussian spatial profile were focused on the sample at the same spot, of 200 μm in diameter. The optimal phase difference used in the experiments was chosen to be similar to that taken from the measured optical poling efficiency dependence *vs.* the phase difference (see the region marked in Fig. 4 of ref. 31). A pair of shutters was used to control the seeding and probing processes. The optically-induced second order susceptibility of the sample was measured by registering the second harmonic generation of the ω beam. During the reading process the 2ω beam was blocked and only the ω beam was left, so that its energy and spot size were the same as during the seeding period. The decay of the second harmonic generation was measured using a pulsed irradiation ("dark"), probing with a few single laser shots only, thus, minimizing the influence of the reading beam on the decay process. No photothermal heating of the samples was observed due to the low loading density of the chromophores and the relatively high glass transition temperature for the polycarbonate polymer matrix used.

3 Theory and calculations

The physical origin of all-optical poling is attributed to the orientational hole burning and molecular re-orientation of the azo-dye chromophores in a polymer host matrix. This process can be described by two coupled orientational diffusion equations for the photoexcitation and re-orientation of the azo-dye molecules in the *trans* and *cis* states:[19,20,31]

$$\begin{cases} \dfrac{\partial n_t(\Omega)}{\partial t} = & -\xi I(\theta) n_t(\Omega) + \\ & + \phi \int\int \Phi(\Omega' \to \Omega) I(\theta') n_c(\Omega')\, d\Omega' + \\ & + k_{1,2} \int\int G(\Omega' \to \Omega) n_c(\Omega')\, d\Omega' + \\ & + D_t \nabla^2 n_t(\Omega) \\ \dfrac{\partial n_c(\Omega)}{\partial t} = & -\phi I(\theta) n_c(\Omega) + \\ & + \xi \int\int Q(\Omega' \to \Omega) I(\theta') n_t(\Omega')\, d\Omega' - \\ & - k_{1,2} n_c(\Omega) + \\ & + D_c \nabla^2 n_c(\Omega) \end{cases}, \quad (1)$$

where $n_t(\Omega)$ and $n_c(\Omega)$ are the molecular densities of the *trans* and *cis* isomers, respectively, with a dipole moment direction in the solid angle $\Omega(\theta,\varphi)$. ξ and ϕ are the quantum efficiencies of the *trans* → *cis* and *cis* → *trans* photoisomerizations, respectively. The *cis* → *trans* thermoisomerization is accounted for by the relaxation rates k_1 (inverse of the *cis* isomer lifetime τ_{c1}) and k_2 (inverse of the *cis* isomer lifetime τ_{c2}), which are applicable to different segments of the chromophore population that exhibit different interactions with the surrounding polymer matrix (eqn (1) for each of these fractions is solved separately).[16,17] $G(\Omega' \to \Omega)$ is the probability for the molecules to rotate from Ω' to Ω in the process of the *cis* → *trans* thermal recovery and is assumed to be applicable to both the aforementioned fractions of the chromophore population. $Q(\Omega' \to \Omega)$ and $\Phi(\Omega' \to \Omega)$ are probabilities of the *trans* → *cis* and *cis* → *trans* optical transitions, respectively. D_t and D_c are the thermally induced orientational diffusion constants for the *trans* and *cis* isomers, respectively.

The first term in eqn (1) (upper) and the second term in eqn (1) (lower) define the photoisomerization of the *trans* → *cis* state. The photoisomerization from the *cis* → *trans* state is described by the first term in eqn (1) (lower) and the second term in eqn (1) (upper). The third term stands for the thermally-induced

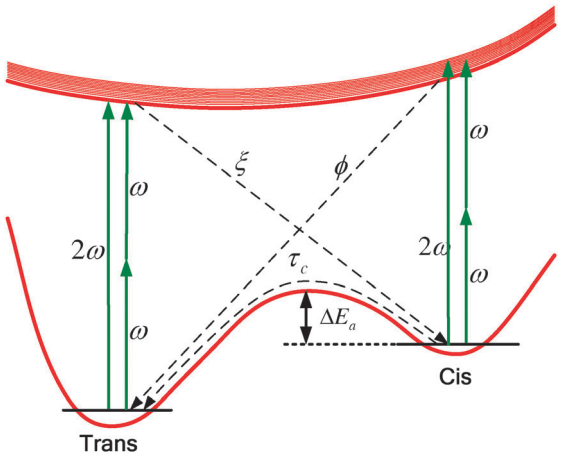

Fig. 4 Simplified scheme of transitions.

relaxation of a *cis* isomer back to the *trans* state. Finally, the fourth term stands for the molecular orientational diffusion. The processes described by eqn (1) correspond to a transition scheme depicted in Fig. 4.

The orientational hole burning mechanism for a *trans* isomer in an all-optical poling is represented by the term $I(\theta)n_t(\Omega)$, where $I(\theta)$ is the excitation rate of the azo-dye molecules:

$$I(\theta) = I_1 \cos^2\theta + I_2 \cos^4\theta + I_3 \cos^3\theta, \quad (2)$$

where

$$I_1 \propto \mu_{01}{}^2 |E_{2\omega}{}^2|,$$

$$I_2 \propto \frac{\mu_{01}{}^2 \Delta\mu^2}{(2\hbar\omega)^2} |E_\omega{}^4|,$$

$$I_3 \propto \frac{\mu_{01}{}^2 \Delta\mu}{\hbar\omega} |E_\omega{}^2 E_{2\omega}{}^* \cos(\Delta\Psi + \Delta kz)|,$$

and where μ_{01} is the transition dipole moment and $\Delta\mu_0 = \mu_1 - \mu_0$ is the difference between the dipole moments in the excited and ground states for a two-level molecule approximation of a rod-like azo-dye chromophore.[28] The parameters I_1, I_2, I_3 correspond, respectively, to the excitation terms of a one-photon absorption at the frequency 2ω (electric field amplitude $E_{2\omega}$), a two-photon absorption at the frequency ω (electric field amplitude E_ω) and the interference between these two terms. $\Delta\Psi$ corresponds to the phase difference between the two beams on the incident surface of the sample. $(\Delta\Psi + \Delta kz)$ is the relative phase between the two beams after propagation over the distance z. The term containing $I_3 \cos^3\theta$ bears a polarity, which is the origin of the photoinduced polar non-centrosymmetry.[28,29]

In a simple case of rod-like molecules of the *trans* isomer and ball-like molecules of the *cis* isomer excited by linearly polarized seeding beams at frequencies ω and 2ω, the all-optical poling process preserves the symmetry around the polarization axis. As a consequence, the angular distributions $n_t(\Omega)$ and $n_c(\Omega)$ depend only on the polar angle θ relative to the polarization axis and can be expanded using Legendre polynomials $P_j(\cos\theta)$ by introducing expansion coefficients T_j and C_j called the order parameters for the *trans* and *cis* isomers, respectively:[19,20]

$$n_t(\Omega) = n_t(\theta) = \frac{1}{2\pi} \sum_{j=0}^{\infty} \frac{2j+1}{2} T_j P_j(\cos\theta), \quad (3)$$

$$n_c(\Omega) = n_c(\theta) = \frac{1}{2\pi} \sum_{j=0}^{\infty} \frac{2j+1}{2} C_j P_j(\cos\theta), \quad (4)$$

The probabilities of the orientational redistribution $G(\Omega' \to \Omega)$, $Q(\Omega' \to \Omega)$ and $\Phi(\Omega' \to \Omega)$ depend only on the rotation angle χ between the directions Ω' and Ω, therefore these functions can also be expanded in terms of the Legendre polynomials $P_j(\cos\chi)$.[19,20]

$$G(\Omega' \to \Omega) = G(\chi) = \frac{1}{2\pi} \sum_{m=0}^{\infty} \frac{2m+1}{2} G_m P_m(\cos\chi), \quad (5)$$

$$Q(\Omega' \to \Omega) = Q(\chi) = \frac{1}{2\pi} \sum_{n=0}^{\infty} \frac{2n+1}{2} Q_n P_n(\cos\chi), \quad (6)$$

$$\Phi(\Omega' \to \Omega) = \Phi(\chi) = \frac{1}{2\pi} \sum_{k=0}^{\infty} \frac{2k+1}{2} \Phi_k P_k(\cos\chi), \quad (7)$$

where G_m, Q_n and Φ_k describe the shape of the probability functions. In order to reduce the complexity of the equations and to make the simulations more ostensive, one of numerous approximations of angular redistribution probability functions can be used.[32] For the azo-dye molecules studied here, it can be assumed that the long molecular axis of each azo-dye molecule is reoriented by a fixed angle α with a random equiprobable azimuth angle η, around the initial orientation (distribution on a cone, Fig. 5).

This leads to a conical redistribution process with $G(\Omega' \to \Omega)$, $Q(\Omega' \to \Omega)$ and $\Phi(\Omega' \to \Omega)$ within the *trans* → *cis* and *cis* → *trans* photoisomerization and *cis* → *trans* thermoisomerization that is given by:[33]

$$G^{ct}(\Omega' \to \Omega) = \Phi^{ct}(\Omega' \to \Omega) = Q^{tc}(\Omega' \to \Omega) = \frac{\delta(\chi - \alpha)}{\sin\alpha}, \quad (8)$$

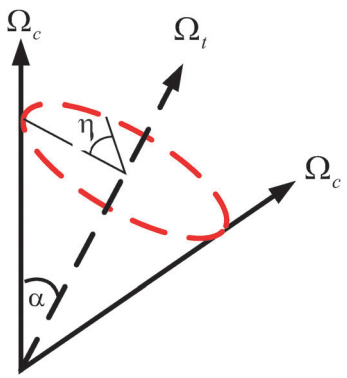

Fig. 5 Schematic drawing of the conical redistribution of the azo-dye molecules by the angle α during isomerization. Ω_t and Ω_c represent the orientation of the long molecular axis for the *trans* and *cis* isomers, respectively.

where $\delta(\chi - \alpha)$ is the delta distribution centered on the angle α. With this distribution G_m, Q_n and Φ_k are simply given by the second-order Legendre polynomial of $\cos\alpha$. For simplicity, we assume that the vector of the transition dipole turns through the same angle both in consequence of the *trans* → *cis* and *cis* → *trans* photoisomerizations, as well as the *cis* → *trans* thermoisomerization processes.

In the case of an assembly of non-interacting molecules, the macroscopic polarizability can be theoretically obtained from the corresponding microscopic polarizability after averaging over all the possible orientations for both fractions of the chromophores, that is,

$$\chi^{(2)} = \int n_t(\Omega)\, d\Omega, \qquad (9)$$

where $n_t(\Omega)$ is the *trans* isomer density oriented in the solid angle Ω. Considering the azo-dye polymeric system dominated by rod-like molecules of the *trans* isomer, the induced $\chi^{(2)}$ can be expressed in terms of the *trans* isomer order parameters T_j.[19,20,31]

In order to model the experimental data eqn (1) is converted into a system of 10 ordinary differential equations for the order parameters T_0, T_1, T_2, T_3, T_4 for the *trans* and C_0, C_1, C_2, C_3, C_4 for the *cis* isomers, respectively, using eqn (3)–(8) for sets of orthogonal Legendre polynomials up to the fourth order. The system was solved and fitted to the experimental data using Matlab software for the CW (continuous wave) excitation case. It was assumed that before the start of the poling process all the azo-dye molecules are in the *trans* isomer state and oriented isotropically. The initial values of the parameters required for the numerical simulation were chosen close to the real ones obtained in our previous experiments with azo-dye doped polymer glasses.[30] It was assumed that the orientational diffusion coefficients for the *trans* and *cis* isomer D_t and D_c, respectively, are equal. In order to verify the predictions made by the model, simulation results were contrasted to experimental all-optical poling transients of azophenylcarbazole **3** and **4** doped polycarbonate measured in a broad range of temperatures.

4 Results

All-optical poling transients measured at different temperatures for two different azophenylcarbazole based chromophores (samples **3** and **4**) in a polycarbonate matrix using the same excitation condition (pulse energy) for the seeding and reading are shown in Fig. 6 and 7. Experimental investigations revealed an accordance between the strength of the optical absorbance and the efficiency of the optical poling for the azophenylcarbazoles in polycarbonate with the most significant effect noted for the chromophore with the highest branched donor (see Fig. 2 in ref. 29 and Fig. 3). Regardless of the embranchment of the azo-dye molecules, poling proceeds in a quite similar way and reaches saturation after ~10 min regardless of the sample temperature. The saturation informs us about some quasi-stationary situation, when the balance between the poling and depoling processes sets in, *i.e.* the photoinduced *trans* → *cis*

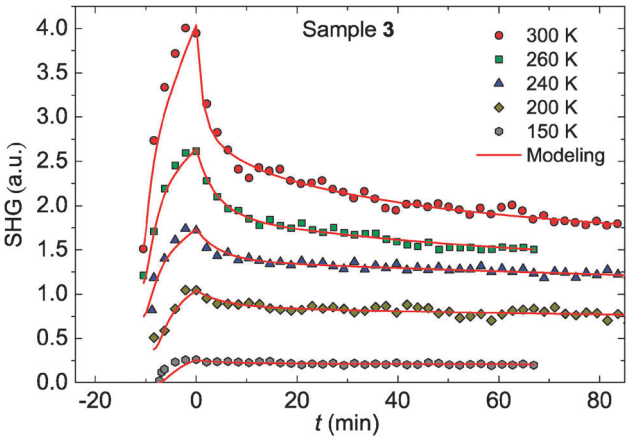

Fig. 6 Second harmonic radiation generated by the optically poled azophenylcarbazole sample **3** at different temperatures (seeding beam: $I_{1\omega}$ = 2.3 J cm^{-2}, $I_{2\omega}$ = 1.7 mJ cm^{-2}; reading beam: $I_{1\omega}$ = 2.3 J cm^{-2}) (''dark'' regime for reading process) (normalized signal, dependencies at different temperatures are offset for clarity). The lines are the modeling results of the induced second order susceptibility tensor component according eqn (1) explained in the section 'Theory and calculations'.

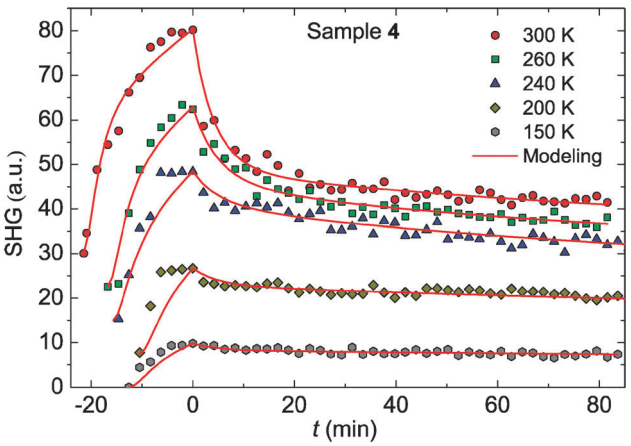

Fig. 7 Second harmonic radiation generated by the optically poled azophenylcarbazole sample **4** at different temperatures (seeding beam: $I_{1\omega}$ = 1.1 J cm^{-2}, $I_{2\omega}$ = 0.73 mJ cm^{-2}; reading beam: $I_{1\omega}$ = 1.1 J cm^{-2}) (''dark'' regime for reading process) (normalized signal, dependencies at different temperatures are offset for clarity). The lines are the modeling results of the induced second order susceptibility tensor component according eqn (1) explained in the section 'Theory and calculations'.

transition and reorientation rate approaches the decay rate of the non-centrosymmetric polar order defined by the thermal and photoinduced *cis* → *trans* transition and, to a lesser extent, the random orientational diffusion of the molecules in the *trans* and *cis* states. The second harmonic generation efficiency strongly depends on the embranchment of the azo-dye molecules, as evidenced by the significantly stronger second harmonic signal for sample **4**. The higher signal value for the more branched chromophore **4** may be explained by a larger partial volume and dipole moment of the molecule, considering its higher polarizability. After poling is stopped, a domain characterized by a relatively fast relaxation occurs, which is related to

the thermal back-reaction of the *cis* → *trans* isomerization, and is present for both samples under investigation. This process cannot be adequately described by a single lifetime. The much slower second time domain concerns mainly the loss of the induced polar order by the thermally induced orientational diffusion. The theoretical model developed was tested for azophenylcarbazole doped polycarbonate by fitting the experimental results to the experimental data. The theoretical simulation results superimposed upon the experimental data are shown in Fig. 6 and 7. The best fit simulation results of the decay transients validate that the thermal *cis* → *trans* isomerization process comprises a composition of two different isomerization reaction rates. A fraction $x = 0.15$ decays with a fixed relaxation rate k_1 (that corresponds to a lifetime of $\tau_{c1} = 300$ s). For both samples x and k_1 are constant and do not show any dependence on temperature in the range under investigation. The remaining fraction $(1 - x) = 0.85$ of all the *cis* isomers decay with a temperature dependent relaxation rate k_2. These two thermoisomerization rates can be attributed to different mobility restrictions of chromophores entrapped in different conformations with the surrounding glassy polymer matrix. Simulation results also indicate that the orientational diffusion rate is significantly slower than the rates associated with the *cis* → *trans* thermoisomerization and is found to be lower for sample **4**, with the more branched chromophore side chains.

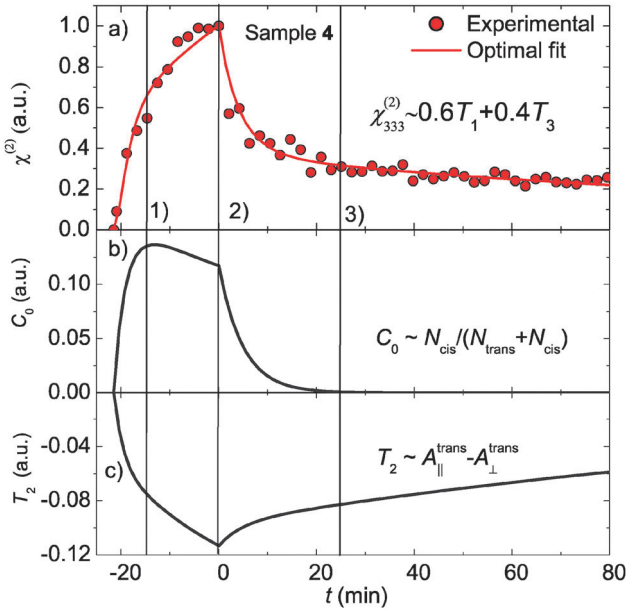

Fig. 8 (a) Temporal dependence of the second harmonic radiation generated by the optically poled azophenylcarbazole sample **4** at 300 K and fitted using an induced second order susceptibility tensor component $\chi^{(2)}_{333}$ (proportional to the order parameters T_1 and T_3) according to the equation shown as an inset. (b) Temporal dependence of the order parameter C_0, obtained as part of the solution to eqn (1), proportional to the relative density of the chromophores in the *cis* state. (c) Temporal dependence of order parameter T_2, obtained as part of the solution to eqn (1), proportional to the orientational anisotropy of the chromophores in the *trans* state.

5 Discussion

5.1 The seeding process

The experimental data and theoretical modeling results indicate that the seeding of the second order nonlinear optical susceptibility gratings in an all-optical poling experiment for the samples investigated can be decomposed as a sum of two contributions: (i) due to an orientational selective *trans* → *cis* photoisomerization that leads to orientational hole burning, and (ii) due to the reorientation of the *trans* isomers during repeated *trans* → *cis* → *trans* photoisomerization cycles.

The superposition of these processes gives rise to a subtle discontinuity of the rate of optical poling (Fig. 8(a), time 1), which can be observed in the experimental transients displayed in Fig. 6 and 7. The dynamics of a typical seeding process is shown in Fig. 8(a), where the temporal dependence of $\chi^{(2)}_{333}(t) \sim \frac{3}{5}T_1(t) + \frac{2}{5}T_3(t)$ (the expression is valid for a system of one-dimensional molecules with bulk azimuthal symmetry[34]) is compared to other coupled order parameters extracted from the numerical solution of eqn (1): (b) C_0, which is proportional to the relative density of the chromophores in the *cis* state and (c) T_2, which is proportional to the orientational anisotropy of chromophores in the *trans* state, represented by the difference in the absorbance of light, polarized parallel ($A\parallel$) and perpendicular ($A\perp$) to the initial all-optical poling direction. It has been observed (Fig. 8(b), up to time 1), that a rapid *trans* → *cis* photoisomerization determines the initial rise of the SHG signal, however, by the time that the density of the chromophores in the *cis* state has reached a dynamic equilibrium, the SHG signal manages to achieve ~50% of its saturation value.

A further rise in the SHG signal (Fig. 8, interval 1 → 2) is governed mostly by the reorientation of the *trans* isomers during repeated *trans* → *cis* → *trans* photoisomerization cycles. Due to the orientation dependence of the rate of photoisomerization cycles, this process also produces a non-centrosymmetric alignment – there is statistical pressure for the *trans* isomers to align perpendicular to the polarization of the poling beams and the molecules that experience isomerization at the highest rate are most likely to be realigned. This process is related to the orientational anisotropy of azo-dyes, governed by the order parameters T_2 and C_2 (Fig. 8(c)). The realignment of the *trans* isomers is further evidenced by the decrease of the dynamic equilibrium value of the relative molecular density of the *cis* isomers during the later stages of seeding (Fig. 8(b), interval 1 → 2).

5.2 The reading process

As in the case of seeding, the second order nonlinear susceptibility grating relaxation process of azophenylcarbazoles is roughly split into two time periods: (i) short – determined by the two distinct rates of the *cis* → *trans* thermoisomerization, k_1 and k_2 (Fig. 8, interval 2 → 3 and Fig. 9, top), and (ii) long – fully determined by the orientational diffusion rate of the *trans* isomers characterized by $k_3 = D_t$ (Fig. 9, bottom). The relative influence of these two relaxation processes is determined by the probabilities of angular redistribution $G(\Omega' \rightarrow \Omega)$, $Q(\Omega' \rightarrow \Omega)$ and $\Phi(\Omega' \rightarrow \Omega)$ – an increased probability of the orientational

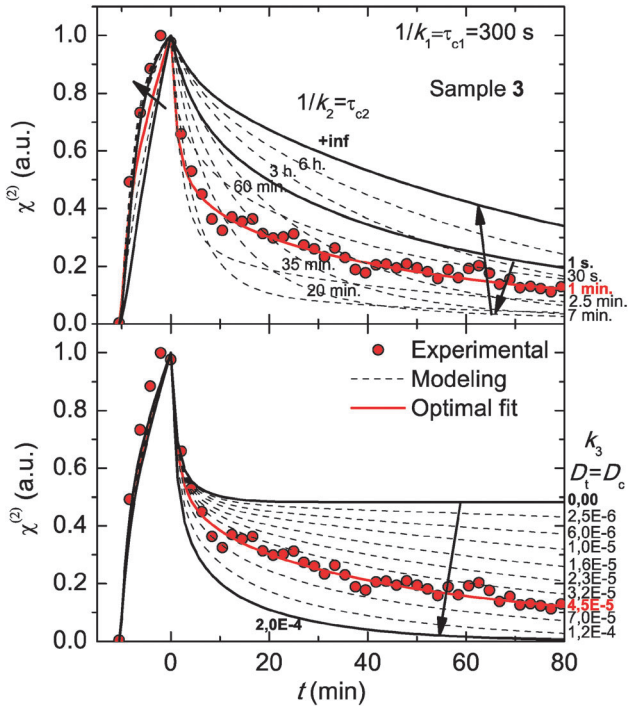

Fig. 9 Relaxation rate of the *cis* isomer $\left(k_2 = \frac{1}{\tau_{c2}}\right)$ dependent (top) and thermal-induced orientational diffusion rate ($k_3 = D_t = D_c$) dependent (bottom) variations of the induced second order susceptibility tensor component $\chi^{(2)}_{333}$ simulation results (lines) compared to the second harmonic radiation generated by the optically poled azophenylcarbazole sample **3** measurement results at 300 K temperature (dots).

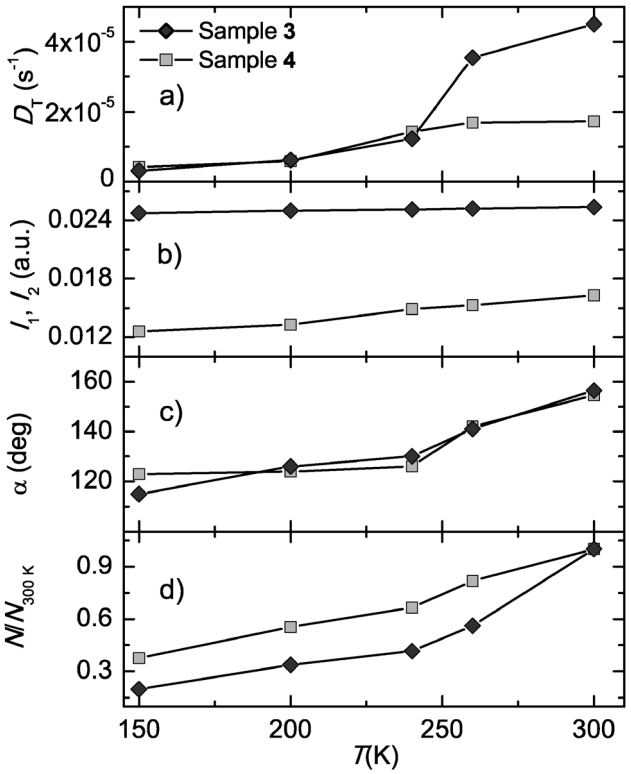

Fig. 10 Temperature dependencies of the parameters used for modeling the experimental optical poling kinetics displayed in Fig. 6 for sample **3** and Fig. 7 for sample **4** according eqn (1). (a) The orientational diffusion coefficient for the *trans* isomers (D_t). (b) Excitation terms of the one-photon absorption at the frequency 2ω (I_1) and the two-photon absorption at frequency ω (I_2) which during this experiment were maintained equal. (c) The most probable azo-dye molecule reorientation angle (α). (d) Density of the active chromophores relative to their density at T = 300 K (N/N_{300K}).

redistribution for the *trans* isomers leads to an increased residual non-centrosymmetry after the rapid *cis* → *trans* thermoisomerization has run its course. This underlies the dependence of transients on the history of the seeding process (a ''memory'' effect related to the seeding conditions) that was reported in ref. 35.

The composite nature of the relaxation process is further evidenced by taking into account the simulation results of the temporal dependence of $C_0(t)$, proportional to the relative density of chromophores in the *cis* state, and the temporal dependence of the order parameter T_2, proportional to the orientational anisotropy of the chromophores in the *trans* state (Fig. 8). The initial rapid relaxation of the SHG signal mirrors the decrease in the relative population of the *cis* isomers (Fig. 8(b), interval 2 → 3). After the density of the *cis* isomers has become negligible, the relaxation is determined by the orientational diffusion rate of the non-centrosymmetrically aligned *trans* isomers $k_3 = D_t$ (Fig. 8(a), from 3 onward).

5.3 Temperature dependence of parameters

The parameters used for fitting the experimental data to the solutions of eqn (1) represent the microscopic characteristics of the azo-dye molecule and its interaction with the surrounding polymer matrix and can be used to quantitatively compare the two systems of azophenylcarbazole-based dyes with side-chains of different embranchment. The temperature dependencies of these fitting parameters are displayed in Fig. 10 and 12. The investigation of the samples in the 150–300 K temperature range, far below T_g, was motivated by the β process, which for a polycarbonate manifests at a temperature of 233 K.[36]

In a realistic azo-dye doped polymer system, the most probable azo-dye molecule reorientation angle α used for the numerical simulation assuming a conical redistribution model, averages over a multitude of all the possible isomerization processes as well as the movements and conformational changes associated with them. For that reason the averaged microscopic probabilities of the orientational redistribution $G(\Omega' \rightarrow \Omega)$ tend to represent the macroscopic orientational distributions of the entire ensemble of the chromophores. In the case of a typical optically induced anisotropy experiment, the chromophore molecules would be reoriented towards the direction perpendicular to the polarization of the incident light, so that an orientational distribution akin to that displayed in Fig. 11(a) is established. This results in the appearance of two ''magic angles'', which were reported for simulations of photo-induced dichroism in azo-polyglutamate films.[33] In the case where additionally the centrosymmetry of the orientational distribution of chromophores is broken (as is the case in our all-optical poling by way of the orientational hole burning) the

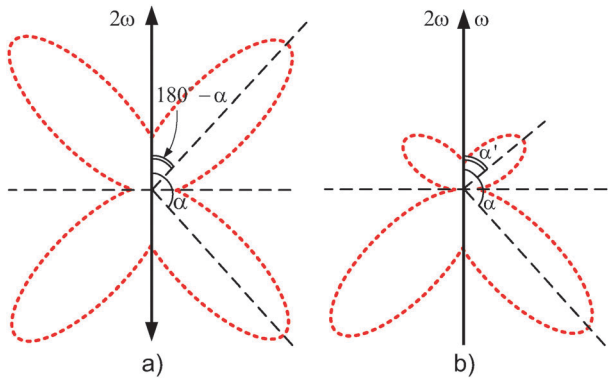

Fig. 11 Simplified polar representation of the orientational distribution of the azo-dye *trans* isomers. (a) The orientational distribution of azo-dye *trans* isomers after the establishment of photoinduced anisotropy. (b) The orientational distribution of the azo-dye *trans* isomers after the establishment of photoinduced anisotropy and non-centrosymmetry in the course of an all-optical experiment.

orientational distribution is similarly deformed (Fig. 11(b)),[37] so that the emergence of a computationally preferred angle α results.

In our case the most probable azo-dye molecule reorientation angle α used for the numerical simulation assuming a conical redistribution model falls within the interval [110;160] deg (Fig. 10(c)). As the samples are cooled, the most probable azo-dye molecule reorientation angle α slowly decreases, which would indicate that at lower temperatures the efficiency of the orientational hole burning and the associated centrosymmetry breaking decreases.

The rates of the three relaxation processes predicted by the model were extracted from the experimental all-optical poling transients of the azophenylcarbazole–polycarbonate guest–host system. The three relaxation rates exhibit diverse temperature dependent behaviors: (i) the two lowest relaxation rates k_2 and k_3 manifest Arrhenius type dependencies, where processes with lower relaxation rates exhibit lower values of the activation energy, (ii) the highest relaxation rate k_1 shows a temperature dependence that is non-Arrhenius, or undistinguished for our experimental conditions.

The temperature dependencies of the relaxation rates k_1 and k_2 provide an insight into the mechanism of activation for the *cis* → *trans* thermoisomerization. The former (k_1) is attributed to a fast non-thermally driven *cis* → *trans* isomerization process, explained by a local structural relaxation mechanism.[17] Initially the environment of the photoexcited *cis* isomer is considered to still be "adjusted" to the geometry of the *trans* isomer, thus the probability of back reaction *cis* → *trans* is the highest. Later on, in the course of the structural relaxation, the surrounding matrix readjusts to the geometry of the *cis* isomer and the probability for the *cis* → *trans* relaxation decreases. The *cis* isomer ends up in a compact temperature sensitive environment, and the *cis* → *trans* thermoisomerization proceeds at the rate of k_2. Thus, the relaxation rate follows an Arrhenius type temperature dependence with an activation energy of 156–157 meV, which was observed for both azophenylcarbazole dye systems under investigation.

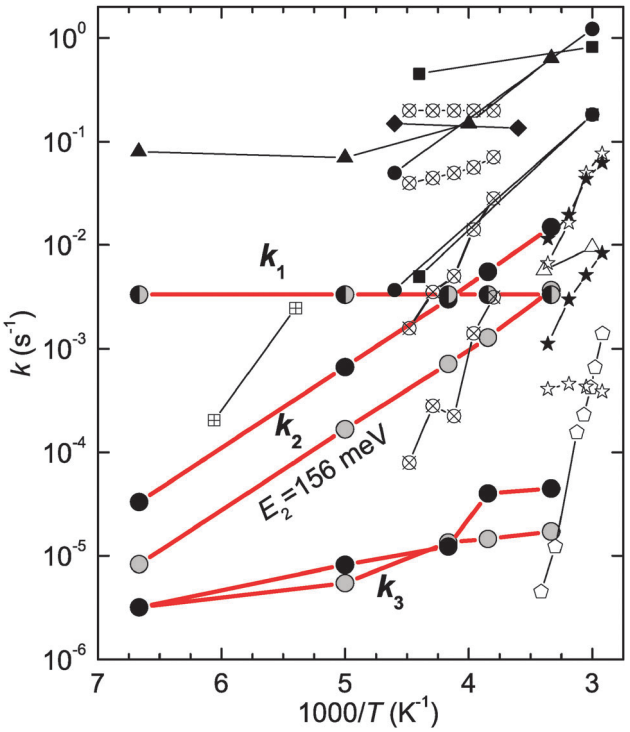

Fig. 12 Relaxation rate constants (k_1, k_2, k_3) obtained from modeling the experimental optical poling kinetics of azophenylcarbazole in a polycarbonate displayed in Fig. 6 (black filled circle) and Fig. 7 (grey filled circle) according to eqn (1) and fitted to an Arrhenius type dependence (the lines in bold are guides for the eye) with a comparison to similar rate activation results presented in the literature: fast and slow rate constant components of Dispersed Red 1 doped hybrid polymer of different rigidity (direction of increase), BM (filled square) > TM (filled circle) > MZ (filled rhomb)[16] and TM (filled triangle);[38] (crossed circle) azobenzene derivative (NAMB) in polymethacrylate (PEMA) measured at 73–113 K below T_g;[17] fast and slow rate constant components of Dispersed Red 1 doped polymethyl methacrylate (PMMA) measured at 20–65 K below T_g (filled star) and Dispersed Red 19 functionalized polyimide polymer measured at 120–165 K below T_g (open star),[39] (open triangle);[19] (crossed square) azobenzene derivative TBA adsorbed on an Au(111) surface;[14] (open pentagon) azobenzene group covalently attached to polyethylene (PE) film measured above T_g ($T_g < T < T_m$).[40]

A comparison of the temperature dependencies of relaxation rates measured in similar systems reported by other groups is given in Fig. 12. Our results correspond well with the relaxation mechanism exhibited by Disperse Red 1 in rigid hybrid polymers, where a relatively lower activation energy was attributed to the rapid (equivalent to k_1) thermoisomerization process.[16] Similar results were published for another guest–host system – Disperse Red 19 dye functionalized polyimide polymer.[19] All the investigations mentioned were performed at temperatures far below T_g. Numerous publications claim that polymers or various other environments provide a catalytic effect for the thermal *cis* → *trans* isomerization.[16] This is in part motivated by the fact that the observed activation energies for polymer guest–host systems are lower compared to solutions. Furthermore, Hagen and co-workers found, that azobenzene derivatives on a Au surface exhibit a thermoisomerization activation energy of 240 meV, which is significantly lower than in solution, yet slightly higher than in a polymer matrix.[14]

In contrast to the conditions of temperatures far below T_g, temperatures above it and particularly in the range $T_g < T < T_m$, resembling the approach to a state of liquid solution with corresponding compactness of the environment, consequently show increased thermoisomerization activation energies (*i.e.* observed by Wang and Weiss in polyethylene films[40]) (see Fig. 12). The lowest relaxation rate component k_3 considered in the model corresponds to the thermal orientational diffusion of the chromophores. A rotational motion responsible for the orientational randomization of ordered *trans* isomers is usually invoked, in order to interpret the slowest decay rates measured either by transient absorption spectroscopy[16] or all-optical poling.[39] Here, it must be stressed that the evaluation of the parameters, which characterize processes that unfold at timescales that significantly exceed the timescales of the experiment, suffer from inevitable inaccuracies. In this particular case, the orientational diffusion rates reported by both groups are, respectively, by almost four and two orders of magnitude higher than ours. By performing the measurements at about ten times longer timescales, we are able to better isolate the three relaxation processes. Thus, regardless of the materials investigated, a reasonable limit for the orientational diffusion rate measurement accuracy has been achieved. Moreover, it corresponds to another limit observed by Wang and Weiss at temperatures above the glass transition. The restrictions for rotation are mainly associated with the rigidity of the chromophore environment. The low rate of the process means that it proceeds mostly after the local structural relaxation has run its course. This implies a temperature driven rotation.

Azo-dye **4** with its higher branching side-chains experiences a stronger interaction with the surrounding polymer matrix, as evidenced by the lower thermal relaxation rate of the *cis* isomer k_2 and a lower rate of orientational diffusion $k_3 = D_t = D_c$ (Fig. 10). Our goal, to investigate a chromophore–polymer system at temperatures in the range of the β transition and below, brought us to a point where the *cis* → *trans* transitions are switched-off and the orientational randomization is suppressed, thus, we observe the chromophores as ''frozen''. Furthermore, our measurements at temperatures around 150 K correspond quite well with the ''frozen'' state observed *via* a photoinduced birefringence for a different dye–polymer system – DR1–hybrid polymer.[38]

6 Conclusions

By introducing a low-temperature all-optical poling investigation we complemented the optical methods used to investigate molecular relaxation mechanisms *via* a gradual switching-off. A model describing all-optical poling transients using a three relaxation rate approach was contrasted to experimental all-optical poling transients of azophenylcarbazole doped polycarbonate measured in a broad range of temperatures and long timescales, thus, enabling to better resolve the different relaxation processes. The relaxation rates k_1 and k_2 describing the *cis* → *trans* thermoisomerization and k_3 – the orientational diffusion of the *trans* isomers exhibited diverse temperature dependent behaviors: the two lowest relaxation rates k_2 and k_3 manifested Arrhenius type dependencies, whereas, the highest relaxation rate k_1 corresponding to a *cis* chromophore lifetime of τ_{c1} = 300 s, showed a temperature dependence that is non-Arrhenius, or undistinguished for our experimental conditions. The activation energy E_{k_2} = 157 meV obtained for both differently branched chromophores speaks about the same thermoisomerization mechanism, though, features a different characteristic lifetime. The investigation of guest–host chromophore–polymer systems at temperatures across the β transition and below led us to uncover the situation when the *cis* → *trans* transitions were switched-off and the orientational randomization was suppressed. Thus, we observed the chromophores as ''frozen''. Altogether, the model, its application to experimental results and the range of conditions used, qualify as extending and complementing the ones observed in numerous other works.

Acknowledgements

This work was partially funded by a grant from the Research Council of Lithuania (project AZOGAN (MIP-078)). The authors wish to express their appreciation to G. Medeišienė for sample preparation.

References

1 M. Williams, R. Landel and J. Ferry, *J. Am. Chem. Soc.*, 1955, **77**, 3701–3707.
2 *The Glass Transition*, ed. E. Donth, Springer Verlag, New York, 2001.
3 *Computational Modeling of Polymers*, ed. J. Bicerano, Marcel Dekker, New York, 1992.
4 G. Adam and J. Gibbs, *J. Chem. Phys.*, 1965, **43**, 139–146.
5 W. Gotze and L. Sjogren, *Rep. Prog. Phys.*, 1992, **55**, 241–376.
6 K. Ngai, *Comments Solid State Phys.*, 1980, **9**, 141–155.
7 P. Debenedetti and F. Stillinger, *Nature*, 2001, **410**, 259–267.
8 A. Buhot and J. Garrahan, *Phys. Rev. Lett.*, 2002, **88**, 225702.
9 N. Metatla and A. Soldera, *Macromolecules*, 2007, **40**, 9680–9685.
10 J. Buchholz, W. Paul and K. Binder, *J. Chem. Phys.*, 2002, **117**, 7364–7372.
11 *Metastable Liquids - Concepts and Principles*, ed. P. Debenedetti, Princeton University Press, Princeton, 1996.
12 *Photochromism - Molecules and Systems*, ed. H. Dürr and H. Bouas-Laurent, Elsevier, Amsterdam, 2003.
13 D. Rais, S. Nešpurek, Y. Zakrevskyy, J. Stumpe, Z. Sedláková and M. Studenovský, *J. Optoelectron. Adv. Mater.*, 2005, **7**, 1371–1375.
14 S. Hagen, P. Kate, M. Peters, S. Hecht, M. Wolf and P. Tegeder, *Appl. Phys. A: Mater. Sci. Process.*, 2008, **93**, 253–260.
15 C. S. Paik and H. Morawetz, *Macromolecules*, 1972, **5**, 171–177.
16 N. Böhm, A. Materny, W. Kiefer, H. Steins, M. M. Müller and G. Schottner, *Macromolecules*, 1996, **29**, 2599–2604.
17 S. Y. Grebenkin and V. M. Syutkin, *Macromolecules*, 2011, **44**, 4538–4545.

18 Z. Sekkat and M. Dumont, *Synth. Met.*, 1993, **54**, 373–381.
19 X. Liu, G. Xu, J. Si, P. Ye, Z. Li and Y. Shen, *J. Appl. Phys.*, 2000, **88**, 3848–3852.
20 G. Xu, X. Liu, J. Si, P. Ye, Z. Li and Y. Shen, *Opt. Lett.*, 2000, **25**, 329–331.
21 X. Yu, X. Zhong, Q. Li, S. Luo, Y. Chen and Y. Sui, *Opt. Commun.*, 2000, **180**, 373–376.
22 B. Guo, F. Guo, Y. Chen, L. Zhu, F. Liu, Q. Zhang and G. Wang, *Chin. Phys. Lett.*, 2006, **23**, 2458–2460.
23 T. Verbiest, D. Burland, M. Jurich, V. Lee, R. Miller and W. Volksen, *Science*, 1995, **268**, 1604–1606.
24 J. Niziol and J. Pielichowski, *Opt. Mater.*, 2010, **32**, 673–676.
25 J. Li, J. Qin and C. Ye, *Synth. Met.*, 2005, **152**, 305–308.
26 L. Zhang, M. Huang, Z. Jiang, Z. Yang, Z. Chen, Q. Gong and S. Cao, *React. Funct. Polym.*, 2006, **66**, 1404–1410.
27 Z. Qin, C. Fang, Q. Pan, Q. Gu, F. Chen, F. Li and J. Yu, *J. Mater. Sci.*, 2002, **37**, 4849–4852.
28 C. Fiorini, F. Charra, J. Nunzi and P. Raimond, *J. Opt. Soc. Am. B*, 1997, **14**, 1984–2003.
29 M. Dumont, *J. Opt. Soc. Am. B*, 2009, **26**, 1057–1075.
30 G. Seniutinas, L. Laipniece, J. Kreicberga, V. Kampars, J. Gražulevičius, R. Petruškevičius and R. Tomašiūnas, *J. Opt. A: Pure Appl. Opt.*, 2009, **11**, 034003.
31 Z. Sekkat and W. Knoll, *J. Opt. Soc. Am. B*, 1995, **12**, 1855–1867.
32 M. Dumont, *J. Opt. Soc. Am. B*, 2011, **28**, 1855–1865.
33 Z. Sekkat, W. Wood and W. Knoll, *J. Phys. Chem.*, 1995, **99**, 17226–17234.
34 M. G. Kuzyk, K. D. Singer, H. E. Zahn and L. A. King, *J. Opt. Soc. Am. B*, 1989, **6**, 742–752.
35 G. Navickaitė, G. Seniutinas, R. Tomašiūnas, R. Petruškevičius, V. Getautis and M. Daškevičienė, *Dyes Pigm.*, 2012, **92**, 1204–1211.
36 M. Parvin and J. G. Williams, *J. Mater. Sci.*, 1975, **10**, 1883–1888.
37 F. Lagugné-Labarthet, C. Sourisseau, R. D. Schaller, R. J. Saykally and P. Rochon, *J. Phys. Chem. B*, 2004, **108**, 17059–17068.
38 N. Böhm, A. Materny, H. Steins, M. M. Müller and G. Schottner, *Macromolecules*, 1998, **31**, 4265–4271.
39 G. Xu, J. Si, X. Liu, Q. G. Yang, P. Ye, Z. Li and Y. Shen, *J. Appl. Phys.*, 1999, **85**, 681–685.
40 C. Wang and R. G. Weiss, *Macromolecules*, 2003, **36**, 3833–3840.

